Measurements of the $\Delta G/G$ at COMPASS

Grzegorz Brona

Warsaw University, Faculty of Physics, 00–681 Warsaw, Poland

ON BEHALF OF THE COMPASS COLLABORATION

The main goal of the COMPASS collaboration at CERN is a quantitative determination of $\Delta G/G$. Three different approaches based on the Photon Gluon Fusion process are utilised. They rely on the PGF tagging via open charm mesons or via high–p_T hadron pairs detection. The latter is measured in the DIS ($Q^2 > 1$ GeV^2) and in the quasi–real photoproduction ($Q^2 < 1$ GeV^2) kinematical regimes. The measurement is done with a two–stage spectrometer capable of particle registration and identification in a wide momentum range. The experiment uses a solid state, polarised ^{6}LiD target and a 160 GeV polarised muon beam.

PACS: 13.60.Hb, 13.85.Hd, 13.88.+e, 14.20.Dh
Key words: COMPASS, deep inelastic scattering, photon gluon fusion, gluon polarization, helicity asymmetry

1 Introduction

In the framework of the QCD, in the light–like gauge, the nucleon spin can be decomposed into four contributions: the contribution from quarks – $\Delta\Sigma$, from gluons – ΔG and from angular momenta of quarks and gluons – L_q and L_g. Therefore the nucleon spin can be presented in the form:

$$\frac{1}{2} = \frac{1}{2}\Delta\Sigma(\mu^2) + \Delta G(\mu^2) + L_q(\mu^2) + L_g(\mu^2) \tag{1}$$

where μ^2 is a scale at which the nucleon wave function is probed [1]. $\Delta\Sigma$ is determined precisely in a QCD fit to the g_1 structure function. However this method gives large uncertainty for ΔG due to the limited kinematical range of the g_1 measurements [2, 3]. ΔG has thus to be measured directly. Up to now its value has been determined by the HERMES [4] and the SMC [5] collaborations in the Photon Gluon Fusion (PGF) process tagged with high–p_T hadron pairs. The primary goal of the COMPASS experiment is to confirm these results and decrease their statistical errors at least by the order of magnitude. Also, for the first time, a direct channel of studying PGF process is utilised. It is based on the PGF tagged with the open charm meson production and decay. The results presented in this paper were obtained from the data coming from 2002-2004 (for the open charm and high–p_T with $Q^2 < 1$ GeV^2 channels) and from 2002-2003 (for the high–p_T with $Q^2 > 1$ GeV^2 channel) periods. Prospects for the 2006 COMPASS data taking are outlined as well.

2 The COMPASS experiment

The COMPASS collaboration consists of more than 250 physicists from 27 institutes from Europe, Russia, Japan and India. The experiment is a result of merging two other originally planned experiments – HMC and Cheops. Consequently the COMPASS physics programme is two–fold. The first part is focused on the spin dependent observables and the second mainly on the hadron spectroscopy. The experiment was approved in 1998 and the spectrometer became operational in 2001 when a commissioning run was taken. In 2002 first physics data with a muon beam were recorded. The muon data taking programme continued in 2003 and 2004. In 2006 the muon programme is resumed after a one year break when the beam was not delivered due to the shutdown of the SPS at CERN.

2.1 The beam

The COMPASS experiment is located in the CERN North Area in the EHN2 hall. It uses a high-intensity muon M2 beam line (Fig. 1). The beam is produced in three subsequent steps. Protons of 400 GeV energy, coming from the Super Proton Synchrotron (SPS), are colliding with a solid 500 mm thick beryllium target (T6) generating a secondary beam which consists mainly of π^+, K^+, π^- and K^- mesons. The positive particles from the beam are then selected with bending magnets and directed into 600 meters long decay tunnel where about 7% of them decay into $\mu^+\nu_\mu$ pairs. At the end of the tunnel a heavy absorber is placed. It stops the remaining hadrons, while μ^+ pass it, loosing only a small fraction of their initial energy. Then the μ^+ beam enters a 400 meters long section where particles of a given energy are selected, and the beam focusing and shaping process takes place with the help of a set of dipole and quadruple magnets (B6–B9). This results in a final μ^+ beam of $\sim$0.8 cm radius at target with $2 \cdot 10^8$ particles per spill (the initial proton spill consists of $1.2{\cdot}10^{13}$ particles). The contamination of hadrons is smaller than 10^{-6}. The spills last 4.8 s each, and are separated by 12 s time windows when the beam is not delivered. The energy of the final beam can be selected in a range of about 60–200 GeV.

Muons coming from the π and K decays are naturally polarised. In the rest frame of the decaying particle muons are 100% polarised and the μ^+ helicity is negative. This fact arises from the angular momentum conservation principle. In a laboratory frame the polarisation of muons is no longer 100%. It depends on the ratio of the muon energy (E_μ) to the decaying meson energy ($E_{\pi,K}$) and is given by the formula:

$$P_\mu = -\frac{m^2_{\pi,K} + (1 - 2E_{\pi,K}/E_\mu)m^2_\mu}{m^2_{\pi,K} - m^2_\mu} \tag{2}$$

Also the cross section for the Photon Gluon Fusion (PGF) process and the experimental acceptance vary with the muon beam energy. Taking into account all the above aspects the beam energy was optimised and has a value of 160 GeV. This corresponds to the polarisation of -0.76 (for 2002 and 2003) and -0.81 (for 2004

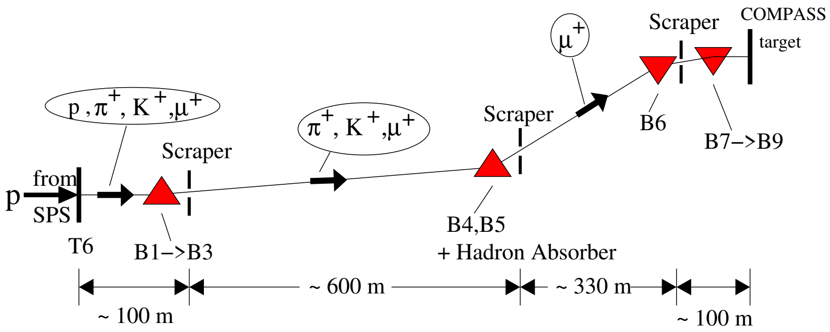

Fig. 1. Sketch of the COMPASS M2 beam line.

when the secondary π, K beam energy was changed). The momenta of the beam particles are measured with the precision of 0.5% with the set of the Beam Momentum Stations (BMS) placed along the beam line. The beam momentum spread is of 3%.

2.2 The target

For the muon programme COMPASS uses a target composed of two cylindrical cells each 60 cm long and 3 cm in a diameter separated by 10 cm gap (cf. Fig. 2). Cells are filled with a solid lithium deuterid, ^{6}LiD. They are located inside a superconducting solenoid which provides a homogenous 2.5 T longitudinal magnetic field. The homogeneity $\Delta B/B$ in the cell region is of the order of $3.5 \cdot 10^{-5}$. The COMPASS solenoid magnet is the one used previously by the SMC collaboration. It provides ± 70 mrad angular acceptance. In 2006 it is replaced by a new one with an aperture of ± 180 mrad [6].

The nuclear spins of the material in both parts of the target are polarised in the opposite directions – parallel and anti–parallel to the magnetic field direction. In order to polarise nuclei a technique based on the Dynamic Nuclear Polarisation phenomenon (DNP) is used. This requires the cells to be enclosed in a microwave cavity and separated by a microwave stopper. Building up the polarisation lasts for about 2 days. The degree of the polarisation is measured using a Nuclear Magnetic Resonance method (NMR). The nucleons that can be polarised make up about 40% of the target material. Its average polarisation obtained was 50%. Directions of the target cell polarisation are flipped every 8 hours by applying an additional magnetic field perpendicular to the target of a maximal induction 0.5 T. The process of the reversal lasts for about 30 minutes and preserves the initial level of polarisation. The twin–target and the spin reversals are needed to cancel false asymmetries

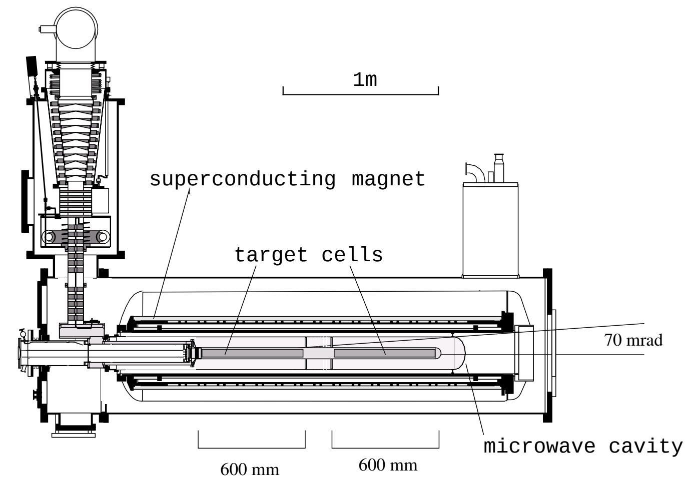

Fig. 2. The setup of the COMPASS target.

originating from different spectrometer acceptances for the two target halves and from the time variations of the beam flux.

2.3 The spectrometer

The COMPASS detector consists of two separate spectrometers – Large Angle Spectrometer (LAS) and Small Angle Spectrometer (SAS) (cf. Fig. 3). This construction allows to perform accurate measurements of tracks of particles emitted at small and large angles with respect to the beam direction. LAS is optimised for angles larger than 30 mrad while SAS is made for small angle, high momentum tracks. Both spectrometers contain dipole magnets, SM1 and SM2, located in LAS and SAS respectively. The first magnet which is located 4 m downstream the target centre has the field integral in the direction along the beam line equal to 1 Tm. Charged particle have to carry momentum larger than 0.4 GeV to be able to cross the magnet and be recorded downstream. The SM2 magnet is located 18 m downstream the target centre and has a field integral of 4.4 Tm. The minimal momentum for charged particles that can pass SM2 is 4 GeV. Zones before and after SM1 and SM2 are equipped with a number of tracking detectors which allow to reconstruct tracks in a magnetic field–free regions. The segments of the reconstructed tracks are then bridged through magnetic field and their 3–momentum vectors are estimated.

The first spectrometer is equipped with a Ring Imaging CHerenkov detector (RICH) responsible for the hadrons identification. It is capable to separate π, K and p in a wide range of momenta starting from a threshold of a few GeV (2.5 GeV, 9 GeV, 17 GeV for π, K and p respectively) up to 43 GeV. Its vessel is 3.3 m long, 6.6 m wide and 5.3 m height (volume of about 80 m^3) and is filled with C_4F_{10} radiator at the atmospheric pressure. The downstream wall of the vessel is covered with 116 hexagonal and pentagonal segments of spherical aluminised mirrors which reflect and focus the Cherenkov photons onto photon detectors located outside the region of the spectrometer acceptance. Multiwire Proportional Chambers with CsI photocatodes are used as photon detectors. They cover an area of 5.3 m^2 and are segmented in 8×8 mm^2 pads which gives a total number of 82 944 pixels. The RICH detector is not well suited for the distinction between pions and muons. Therefore for muon identification the drift tubes detectors installed at the end of LAS and SAS are used. In front of them 60 cm iron and 2.4 m concrete walls are placed respectively. The walls work as filters absorbing all charged particles but muons.

Both spectrometers contain hadronic calorimeters (HCAL1 and HCAL2). They have a sandwich construction of alternate scintillators and iron plates. The task of the hadronic calorimeters is to support the differentiation between the muon and hadron tracks. They are also used in the trigger system. SAS is additionally equipped with an electromagnetic calorimeter (ECAL2) made of lead glass blocks. A second electromagnetic calorimeter (ECAL1) has been added to the experiment setup in 2006.

The data acquisition is started if an event fulfils certain criteria defined by the scattering angle of the muon and by the energy deposited in the hadronic calorimeters. The triggers start data acquisition for events with both quasi–real photons ($Q^2 \ll 1$ GeV^2) and inclusive deep inelastic scattering ($Q^2 > 1$ GeV^2). They are based on four sets of hodoscope detectors which cover different kinematical regions of the interaction. Additionally the information from the hadronic calorimeters is used and the beam halo veto is applied. For 2002–2004 data taking seasons the number of triggers per spill varied from 20 000 to 40 000.

More information on the COMPASS spectrometer can be found in [7].

3 Photon Gluon Fussion

The PGF process is an interaction of a virtual photon coming from the muon with a virtual gluon embedded in the nucleon (Fig. 4). The interaction occurs via the exchange of the virtual quark and results in a $q\overline{q}$ pair production. It gives a direct insight into the gluon distribution in the nucleon. The PGF process was successfully used for the studies of the unpolarised gluon distribution G at HERA [8]. In the COMPASS experiment the same process, but involving polarised target and beam reveals the polarised gluon distribution ΔG.

The COMPASS analysis is based on the measurement of the difference in the cross sections for the PGF interactions occurring with different relative spin orientations

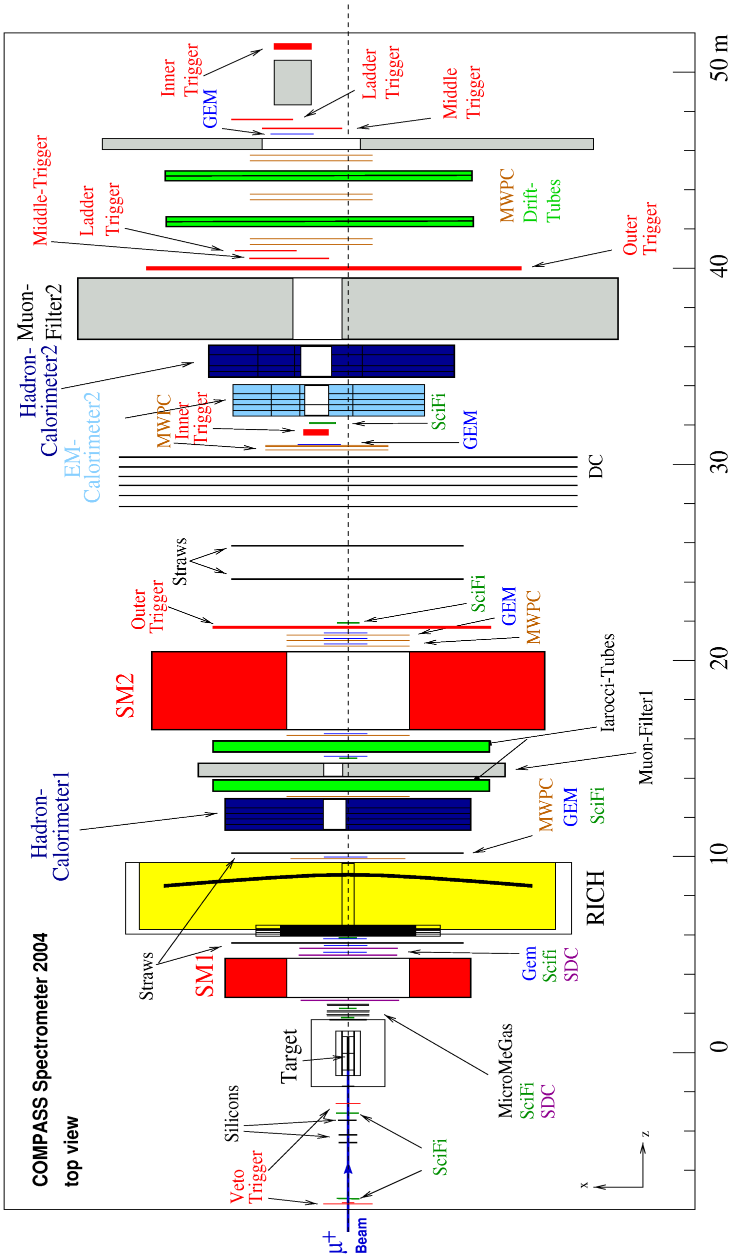

Fig. 3. The COMPASS spectrometer in 2004.

of the projectile and of the target nucleus. If the direction of the former is denoted with $\uparrow$ and the latter with $\Uparrow$ the asymmetry measured by the spectrometer is:

$$A^{exp} = \frac{N_{PGF}^{\downarrow\Uparrow} - N_{PGF}^{\downarrow\Downarrow}}{N_{PGF}^{\downarrow\Uparrow} + N_{PGF}^{\downarrow\Downarrow}} \tag{3}$$

Where N_{PGF} are the numbers of the PGF interactions occurring with different relative target–beam spin orientations. The above experimental asymmetry (A^{exp}) can be translated into the asymmetry of the muon–nucleon interactions ($A^{\mu N}$) by dividing it by several dilution factors. These are: the beam polarisation P_B, the target polarisation P_T and the material dilution factor f. The first two correspond to the corrections due to the beam and target polarisations smaller than 100% while the third factor describes the amount of the polarisable nucleons in the target material:

$$A^{\mu N} = \frac{1}{P_B P_T f} A^{exp} \tag{4}$$

The $A^{\mu N}$ is related to the photon–nucleon asymmetry ($A^{\gamma^* N}$):

$$A^{\gamma^* N} = \frac{1}{D} A^{\mu N} = \frac{1}{P_B P_T f D} A^{exp} \tag{5}$$

where D is a depolarisation factor that describes the fraction of the longitudinal lepton beam polarisation transferred to the virtual photon.

The double target setup with target halves polarised in the opposite directions enable the measurement of the two spin configurations at the same time. Therefore

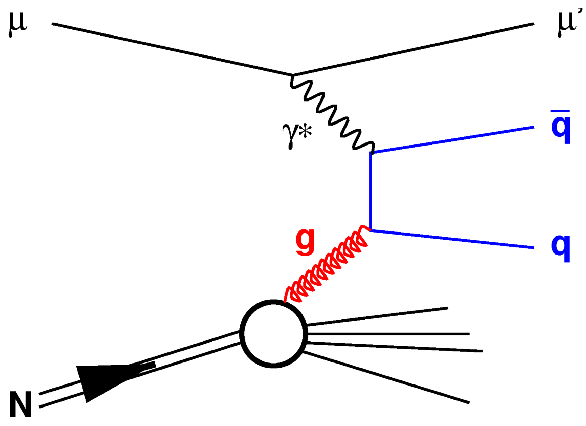

Fig. 4. Photon Gluon Fusion (PGF) process.

the measurement is independent of the total integrated muon flux as well as of its time changes. However the acceptance of the spectrometer for the particle tracks coming from different target cells is not the same. The experimental asymmetry given with Eq. (3) will be sensitive to this difference. Therefore every 8 hours the polarisation of the cells is reversed and the acceptance independent experimental asymmetry can be written as:

$$A^{exp} = \frac{1}{2}\left(\frac{N^{\downarrow\Uparrow}_{PGF} - N^{\downarrow\Downarrow}_{PGF}}{N^{\downarrow\Uparrow}_{PGF} + N^{\downarrow\Downarrow}_{PGF}} + \frac{N'^{\downarrow\Uparrow}_{PGF} - N'^{\downarrow\Downarrow}_{PGF}}{N'^{\downarrow\Uparrow}_{PGF} + N'^{\downarrow\Downarrow}_{PGF}}\right) \tag{6}$$

where each of the two terms correspond to periods with a given spin configuration in the target halves. This method makes the measurement acceptance independent as long as the efficiency of the spectrometer is the same for the data taking before and after the polarisation reversal. The possible effects of the acceptance fluctuations induced by the reversal process are taken into account in the studies of systematic errors.

Two different methods using the PGF mechanism are currently employed by COMPASS. The first one is based on tagging the PGF via the reconstruction of the charmed mesons appearing from the $c\overline{c}$ quark pairs fragmentation. It is called the open charm method as the tagging is focused on the detection of D^0 mesons [10], [11]. The second approach relies on the selection of hadron pairs with high transverse momenta with respect to the virtual photon direction [12]. The advantage of this method is a much higher statistics as it is not restricted only to charmed quark pairs in the final state. However it relies on theoretical assumptions that enter the Monte Carlo generators used for this method.

4 The open charm method

The mass of a charm quark, $m_c \approx 1.5$ GeV, is much larger than these of u, d and s quarks. Therefore the intrinsic charm content of the nucleon is negligible. Also the production of the charm quarks in the fragmentation process is highly suppressed. Thus the only reaction that has a significant contribution to the charm production is PGF. The contribution from the resolved photon processes in the COMPASS kinematics in the charm production is small. The charmed quarks fragment subsequently into charmed hadrons. The detection and identification of them provides a clear tag for the PGF process. From all known charmed hadrons the one that can be most clearly reconstructed in the COMPASS kinematics is a D^0 "open charm" meson. The fragmentation into D^0 is also the process that is quite well understood theoretically, as compared for instance to the fragmentation into charmonia states. On average 1.2 D^0 mesons are produced per each $c\overline{c}$ pair [9].

The open charm mesons are reconstructed through their πK decay channel which has a branching ratio of 3.8%. As there is a strong multiple Coulomb scattering of the charged particles inside the COMPASS solid state target the space resolution of the vertex reconstruction is not enought to separate D^0 production point from its decay vertex. Therefore the mesons are reconstructed on the combinatorial bases, pairing each two charged tracks from a given event and calculating the invariant mass of the system. The disadvantage of the method is a high combinatorial background that has to be reduced with a set of cuts. Among them the most important is the RICH particles identification in case of a kaon candidate. This entails the restriction of the studied sample to the subsample with kaon candidates having momenta larger than the RICH threshold for kaons to radiate the Cherenkov light. In the COMPASS kinematics about 80% of kaons coming from the D^0 decay exceed this threshold. The other important cuts are the selection of the open charm candidates with $z > 0.25$ where z is a fraction of the energy carried by the candidate to the energy of the virtual photon and a cut on the angle between the D^0 flight direction and the momentum vector of the kaon in the cms of the decaying open charm meson, $\cos\theta^*_K < |0.5|$. These cuts reject effectively the combinatorial pairs coming from the nucleon fragmentation region but not from PGF. With these cuts the ratio of the signal events to the background is still small, of the order of 1:10. Therefore, a second, more exclusive, decay channel is studied: $D^* \to D^0\pi \to K\pi\pi$. In this channel a cut on the mass difference can be imposed: 3.1 MeV $< M_{K\pi\pi} - M_{K\pi} - M_\pi <$ 9.1 MeV where the $M_{K\pi\pi}$ is the mass of the D^* candidate and $M_{K\pi}$ is the mass of the D^0 candidate. For this channel the kinematical cuts are fixed to: $z > 0.2$, $\cos\theta^*_K < |0.85|$. The resultant signal to background ratio is approximately 1:1 (cf. Fig. 5).

The $A^{\gamma^* N}$ asymmetry, Eq. (5), can be rewritten in a form:

$$A^{\gamma^* N} = \frac{1}{P_B P_T f D \frac{S}{S+B}} A^{exp} + A^{BG} \tag{7}$$

Where the $S/(S+B)$ is an additional dilution factor with S and B being a number of signal and background events in a studied open charm sample. The A^{BG} is a background asymmetry arising from the other spin dependent processes embedded in the studied sample. These however have a negligible contribution (comparing to the statistical error of the measurement in the open charm channel). With the elementary photon–gluon cross–sections for the helicity dependent and helicity averaged cases, $\Delta\sigma^{\gamma^* g \to c\bar{c}X}(\hat{s})$ and $\sigma^{\gamma^* g \to c\bar{c}X}(\hat{s})$, the virtual photon–nucleon asymmetry takes a form:

$$A^{\gamma^* N} = \frac{\int_{4m_c^2}^{2M\nu} d\hat{s}\ \Delta\sigma^{\gamma^* g \to c\bar{c}X}(\hat{s}) \Delta G(x_g, \hat{s})}{\int_{4m_c^2}^{2M\nu} d\hat{s}\ \sigma^{\gamma^* g \to c\bar{c}X}(\hat{s}) G(x_g, \hat{s})} \tag{8}$$

In the above equations x_g is the gluon momentum fraction while $\hat{s}$ is a photon–nucleon centre of the mass energy squared:

$$\hat{s} = (\mathbf{q} + x_g \mathbf{P})^2 \approx \lim_{Q^2 \to 0} 2 x_g \nu M \tag{9}$$

The integration limits in Eq. (8) are given by the threshold energy for the $c\bar{c}$ production ($2m_c$) and by the total energy available in the interaction for a given ν

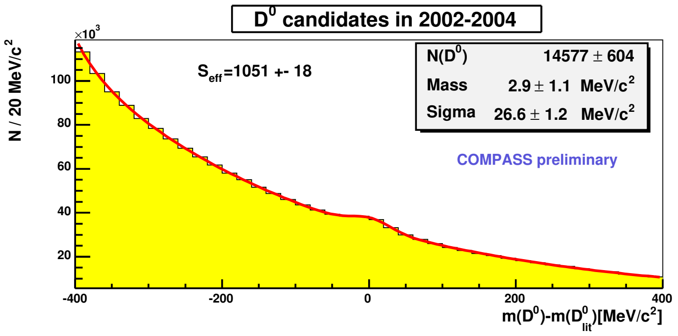

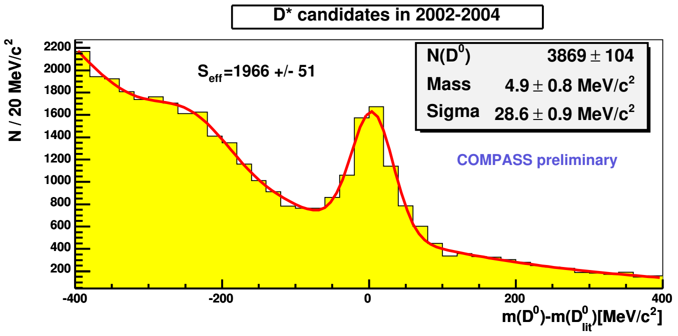

Fig. 5. Distributions of the invariant mass of the πK systems for D^0 untagged and tagged with D^* samples.

($\sqrt{2M\nu}$). The partonic asymmetry for the photon–gluon interaction, $\hat{a}_{LL}$, is defined as:

$$\hat{a}_{LL}(\hat{s}) = \frac{\Delta\sigma^{\gamma^* g \to c\bar{c}X}(\hat{s})}{\sigma^{\gamma^* g \to c\bar{c}X}(\hat{s})} \tag{10}$$

Substituting $\hat{a}_{LL}$ to Eq. (8) one gets:

$$A^{\gamma^* N} = \frac{\int_{4m_c^2}^{2M\nu} d\hat{s}\ \hat{a}_{LL}(\hat{s}) \frac{\Delta G(x_g,\hat{s})}{G(x_g,\hat{s})} \sigma^{\gamma^* g \to c\bar{c}X}(\hat{s}) G(x_g,\hat{s})}{\int_{4m_c^2}^{2M\nu} d\hat{s}\ \sigma^{\gamma^* g \to c\bar{c}X}(\hat{s}) G(x_g,\hat{s})} \tag{11}$$

$$\approx \langle \hat{a}_{LL} \rangle \times \langle \frac{\Delta G}{G} \rangle \tag{12}$$

The above equation together with Eq. (7) and $A_{BG} = 0$ couples the experimental asymmetry with the $\Delta G/G$:

$$\langle \frac{\Delta G}{G} \rangle = \frac{1}{P_B P_T f D \langle \hat{a_{LL}} \rangle \frac{S}{S+B}} A^{exp} \tag{13}$$

The a_{LL} for a given open charm event can be in a range starting from negative values up to 1. Events characterised by different values of kinematical variables and thus different a_{LL} carry different amount of information on the $\Delta G/G$. Therefore the so called weighted method of the $\Delta G/G$ extraction was applied in the COMPASS analysis. In this method each event is weighted taking into account the P_B, f, D and a_{LL} factors. The target polarisation P_T is not used in the weight since it varies with time and therefore may introduce a systematic bias to the final result. The weighted method requires the knowledge of the a_{LL} for each event separately. The a_{LL} can be calculated on an event-by-event bases only if two charmed hadrons are registered in the final state and the whole kinematics of the reaction is known. This is not the case in the COMPASS open charm analysis where the reconstruction of only one charmed meson is required. Thus the parameterisation based on the measured kinematical variables was introduced providing the best estimation of the a_{LL} parameter for each open charm event. The variables that were used are: the fraction of the energy carried by D^0, the transverse momentum of the D^0 with respect to the virtual photon direction and the global variables x, y and Q^2. The parameterisation was obtained using Neural Networks that was taught on a Monte Carlo sample. The sample had been prepared with the AROMA generator in the leading order QCD, processed with a GEANT simulation of the COMPASS detector and reconstructed with the COMPASS track reconstruction software. The correlation between the a_{LL} values coming directly from the generation and reconstructed with the parameterisation is about 82% (cf. Fig. 6).

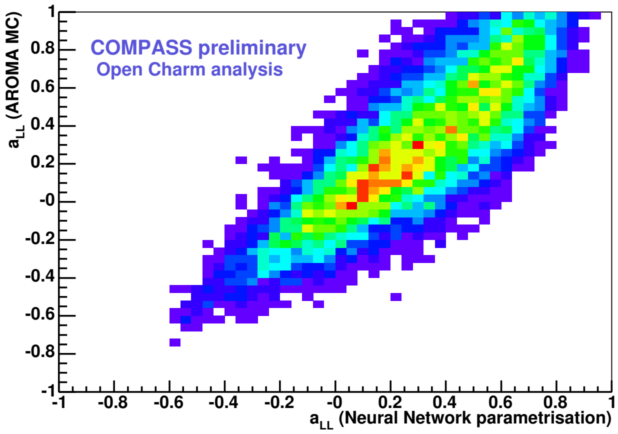

Fig. 6. Correlation between a_{LL} generated and reconstructed using the Neural Network parameterisation of a_{LL}.

The preliminary result from the COMPASS open charm analysis for 2002-2004 data obtained with the weighted method is (cf. Fig. 7):

$$\langle\frac{\Delta G}{G}\rangle = -0.57 \pm 0.41 \text{ (stat)} \tag{14}$$

while the average x_g for the measured sample is 0.15 with RMS of 0.08. The hard scale at which the value was obtained is 13 GeV^2. It is given by the mass of the charm quark and the transverse momentum of D^0 meson: $\mu^2 = 4(m_c^2 + p_t^2)$. Systematic error is still a subject of studies however up to the order of the statistical error no systematic effect was observed.

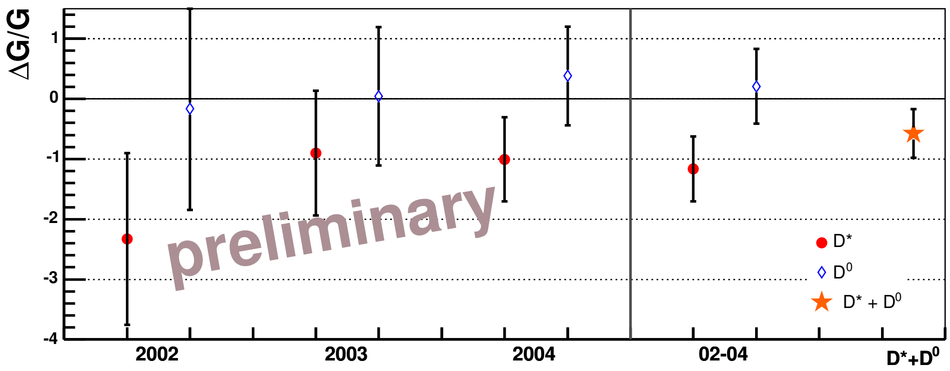

Fig. 7. Values of $\Delta G/G$ calculated for each data taking year separately for D^0 channels tagged and untagged with D^* meson. Also the weighted average for all the years for both channels is presented.

5 The high–p_T method

The second method to study the polarised Photon Gluon Fusion process is the measurement of the asymmetries for events with two hadrons having high transverse momenta relative to the virtual photon direction. In the PGF process and in the $\gamma^* g$ centre of mass quarks are produced back-to-back. In the leading process where a quark is struck directly by a photon it inherits the direction of the momentum from the projectile. After the fragmentation the hadrons usually preserve the direction of motion of the quarks they originate from. Therefore with the selection of two high–p_T hadrons a fraction of PGF events in the studied sample is strongly enhanced and in the COMPASS case reaches about 30%. For the remaining 70% of events the underlying reaction differs from the PGF. The high–p_T analysis is performed in two kinematical regimes: one focuses on the subsample of events with $Q^2 > 1$ GeV^2, the second on the subsample with $Q^2 < 1$ GeV^2. For both the cuts selecting high–p_T hadrons are similar:

- hadron candidates are detected in the hadronic calorimeters and not in the muon detectors located downstream the muon filters;
- $p_{T_1} > 0.7$ GeV and $p_{T_2} > 0.7$ GeV (where p_{T_1} and p_{T_2} are hadrons transverse momenta relative to the virtual photon direction);
- $p_{T_1}^2 + p_{T_2}^2 > 2.5$ GeV;
- invariant mass of the system of two hadrons is larger than 1.5 GeV (this requirement discards the resonance region).

5.1 The high–$\mathbf{p_T}$ method for $\mathbf{Q^2} > 1$ GeV$^\mathbf{2}$

For the high–p_T analysis with $Q^2 > 1$ GeV^2 apart from the PGF the sample contains a large fraction of the leading order DIS processes ($\gamma q \to q$) and QCD–Compton interactions ($\gamma q \to gq$). The fraction of the resolved photon processes in the region of high Q^2 is smaller than 10% and its influence on the measurement can be neglected. With the R_{PGF}, R_{LO} and R_{QCDC} being respectively fractions of events with PGF, leading order and QCD–Compton the double helicity asymmetry reads:

$$A^{\gamma^* N \to hh} = R_{PGF} \langle \hat{a}_{LL}^{PGF} \rangle \frac{\Delta G}{G} + \left[R_{LO} \langle \hat{a}_{LL}^{LO} \rangle + R_{QCDC} \langle \hat{a}_{LL}^{QCDC} \rangle \right] \frac{\Delta q}{q} \tag{15}$$

Here Δq and q are polarised and unpolarised quark distributions. In the analysis performed at COMPASS an additional cut rejecting events with $x > 0.05$ is imposed. In the phase space that is not affected by this cut the measured A_1 asymmetry is small which approximately corresponds to the smallness of the $\Delta q/q$. Therefore the terms describing LO and QCDC interactions can be dropped from the above equation:

$$A^{\gamma^* N \to hh} = R_{PGF} \langle \hat{a}_{LL}^{PGF} \rangle \frac{\Delta G}{G} \tag{16}$$

The R_{PGF} has to be estimated from the Monte Carlo. Therefore its value is model dependent which introduces an additional systematic uncertainty to the analysis. The MC generator used is LEPTO 6.5.1 which describes reasonable well the physics at high Q^2 [13].

A preliminary result from the COMPASS high–p_T analysis from 2002-2003 data at $Q^2 > 1$ GeV^2 is:

$$\langle \frac{\Delta G}{G} \rangle = 0.06 \pm 0.31 \text{ (stat)} \pm 0.06 \text{ (syst)} \tag{17}$$

The fraction of R_{PGF} is equal to 0.34 ± 0.07, the average x_g for the sample is 0.13 with RMS of 0.08 while the hard scale at which the value was obtained is 3 GeV^2. The hard scale is given by the transverse momentum of the outgoing partons. The main contribution to the systematic error comes from the false asymmetries.

5.2 The high–$\mathbf{p_T}$ method for $\mathbf{Q^2 < 1}$ GeV$^\mathbf{2}$.

For the COMPASS experiment the bulk of events containing two high–$\mathrm{p_T}$ hadrons is at small Q^2. About 90% of events have $Q^2 < 1$ GeV^2. In this kinematic region apart from the direct processes (PGF, LO and QCDC) the important part comes from the resolved photon interactions. Their contributions, in contrast to the $Q^2 > 1$ GeV^2 analysis, cannot be neglected as they contribute to more than 50% of interactions. The asymmetry is thus:

$$A^{\gamma^* N \to hh} = R_{PGF} \langle \hat{a}_{LL}^{PGF} \rangle \frac{\Delta G}{G} + \left[R_{LO} \langle \hat{a}_{LL}^{LO} \rangle + R_{QCDC} \langle \hat{a}_{LL}^{QCDC} \rangle \right] \frac{\Delta q}{q} + A_{RP} \quad (18)$$

In the resolved photon interactions a photon fluctuates first into a hadron, then a parton from the hadron interacts with another parton coming from a nucleon. The interaction can occur in a number of channels each having its separate contribution to the $A^{\gamma^* N \to hh}$ asymmetry:

- $qq^\gamma \to qq$ where q is a nucleon quark while q^γ is a resolved photon quark. The contribution from this process to $A^{\gamma^* N \to hh}$ is:

$$R_{qq} \langle \hat{a}_{LL}^{qq} \rangle \frac{\Delta q}{q} \left(\frac{\Delta q}{q} \right)^\gamma \quad (19)$$

- $qg^\gamma \to qg$ where q is a nucleon quark and g^γ is a gluon coming from the hadronic structure of the photon. The contribution is given by:

$$R_{qg} \langle \hat{a}_{LL}^{qg} \rangle \frac{\Delta q}{q} \left(\frac{\Delta G}{G} \right)^\gamma \quad (20)$$

- $gg^\gamma \to gg$ where one gluon comes from the nucleon and another from the resolved photon. The contribution to $A^{\gamma^* N \to hh}$ is equal to:

$$R_{gg} \langle \hat{a}_{LL}^{gg} \rangle \frac{\Delta G}{G} \left(\frac{\Delta G}{G} \right)^\gamma \quad (21)$$

- $q\overline{q}^\gamma \to q\overline{q}$, $\overline{q}q^\gamma \to qq$, $q\overline{q}^\gamma \to gg$, $\overline{q}q^\gamma \to gg$, $gg^\gamma \to q\overline{q}$ processes account for only a very small fraction of high–$\mathrm{p_T}$ events (0.6% in total) and can be neglected.

The total asymmetry produced by interactions involving resolved photons is:

$$A_{RP} = R_{qq} \langle \hat{a}_{LL}^{qq} \rangle \frac{\Delta q}{q} \left(\frac{\Delta q}{q} \right)^\gamma + R_{qg} \langle \hat{a}_{LL}^{qg} \rangle \frac{\Delta q}{q} \left(\frac{\Delta G}{G} \right)^\gamma + R_{gg} \langle \hat{a}_{LL}^{gg} \rangle \frac{\Delta G}{G} \left(\frac{\Delta G}{G} \right)^\gamma \quad (22)$$

Where the superscript γ denotes the parton distributions describing the resolved photon structure. This structure is known only for the unpolarised case: q^γ and G^γ

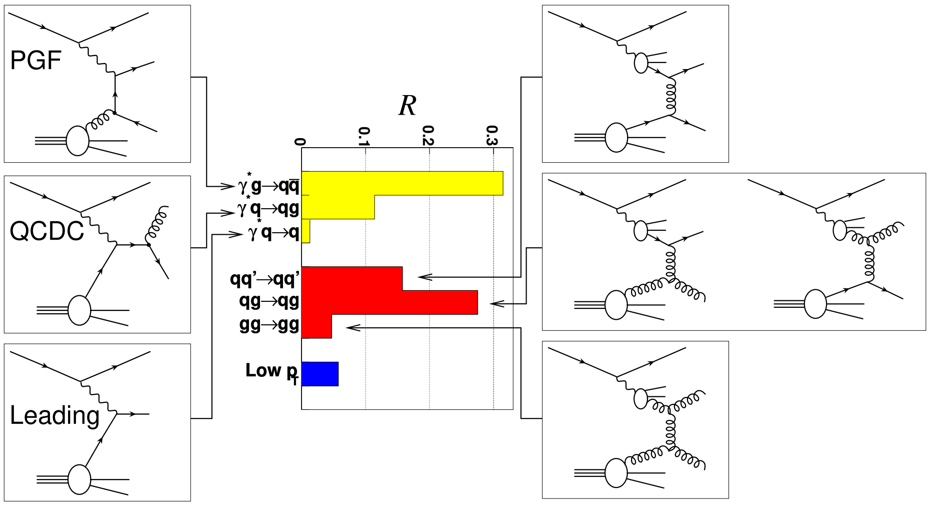

Fig. 8. The contributions of different processes extracted from the PYTHIA Monte Carlo sample of events with $Q^2 < 1$ GeV^2. On the left the direct processes are presented and on the right the resolved photon contributions. Processes with negligible contributions were neglected.

were measured experimentally while the Δq^γ and ΔG^γ polarised distributions are not known. Their magnitudes can only be estimated as theoretical considerations provide a minimum and a maximum values for them [14]. The uncertainty arising from this procedure is included in the systematic error of the final result. As it can be seen from Eq. (22) the resolved photon contributions not only dilute the measured $\Delta G/G$ but also through the $gg^\gamma \to gg$ channel are sensitive to it. Finally the total asymmetry reads:

$$A^{\gamma^* N \to hh} = \Big[R_{PGF}\langle \hat{a}_{LL}^{PGF}\rangle + R_{qg}\langle \hat{a}_{LL}^{gg}\rangle \Big(\frac{\Delta G}{G}\Big)^\gamma\Big]\frac{\Delta G}{G} +$$
$$+\Big[R_{LO}\langle \hat{a}_{LL}^{LO}\rangle + R_{QCDC}\langle \hat{a}_{LL}^{QCDC}\rangle + R_{qq}\langle \hat{a}_{LL}^{qq}\rangle \Big(\frac{\Delta q}{q}\Big)^\gamma + R_{qg}\langle \hat{a}_{LL}^{qg}\rangle \Big(\frac{\Delta G}{G}\Big)^\gamma\Big]\frac{\Delta q}{q} \quad (23)$$

The fractions of the processes as well as the average a_{LL} for each process have to be estimated with a Monte Carlo. The large number of parameters not measured directly but estimated from the simulation results in a strong model dependence of the resultant $\Delta G/G$ value. This dependence is encompassed in a systematic error. The generator that was used for the $Q^2 < 1$ GeV^2 sample is PYTHIA 6.2 [15].

The result from COMPASS high–$\mathrm{p_T}$ analysis from the 2002-2003 sample of $Q^2 <$

1 GeV^2 data is:

$$\langle\frac{\Delta G}{G}\rangle = 0.024 \pm 0.089\ (\mathrm{stat}) \pm 0.057\ (\mathrm{syst}) \tag{24}$$

The average x_g is $0.095^{+0.08}_{-0.04}$ and the hard scale is equal to 3 GeV^2 [16]. The hard scale is given by the transverse momentum of the outgoing partons. The systematic error includes the experimental systematic, uncertainty arising from the applied Monte Carlo procedure and the estimate of the resolved photon contribution. The preliminary result for the whole 2002-2004 data set is:

$$\langle\frac{\Delta G}{G}\rangle = 0.016 \pm 0.058\ (\mathrm{stat}) \pm 0.055\ (\mathrm{syst}) \tag{25}$$

With the same x_g and the same scale.

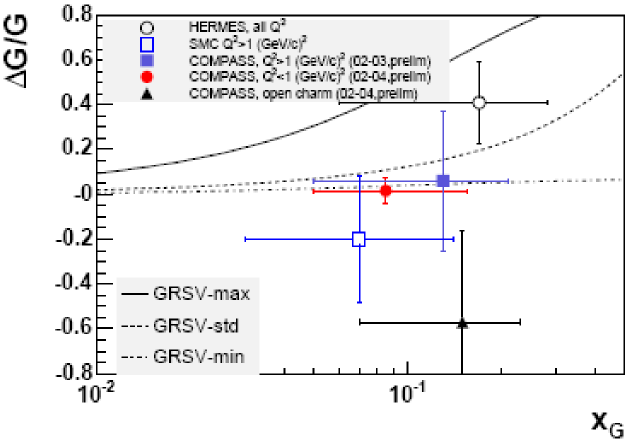

Fig. 9. Comparison of the $\Delta G/G$ measurements from COMPASS, SMC [5] and HERMES [4]. The horizontal bar at each point corresponds to the range in x_g of the measurement. The curves show the GRSV2000 [17] parameterisations at 3 GeV^2 and in the $\overline{\mathrm{MS}}$ scheme for the minimal, maximal and best fit scenarios. Note that COMPASS open charm point was obtained at a much higher hard scale.

6 Summary

In Fig. 9 the results obtained with three different approaches are summarised and compared with the parton parameterisations evaluated at the scale of 3 GeV^2 in the $\overline{\mathrm{MS}}$ scheme [17]. Three curves are plotted for the maximal, best fit and minimal scenarios (for details see [16] or [17]). They correspond to the x_g integrated ΔG values of 2.5, 0.62 and 0.16, respectively. While the results coming from high–$\mathrm{p_T}$

analysis were obtained for the scale of the parameterisation, the value from the open charm channel was extracted at much higher one. Both COMPASS high–p_T results favour small values of ΔG. However at the level of the measurement precision the scenarios with large ΔG cannot be ruled out. At the plot also the results from HERMES [4] and SMC [5] high–p_T analysis are presented. In comparison with them the COMPASS result for $Q^2 < 1$ GeV^2 has a much smaller uncertainty while the one for $Q^2 > 1$ GeV^2 is at the same level of precision. The value coming from the open charm channel has the largest statistical error, however this measurement is the most direct one, since it is only weakly based on Monte Carlo models. It should also be stressed that it is the only such measurement performed up to now. Its value within the error is compatible with zero.

7 Prospects

The COMPASS experiment in 2002-2004 data taking periods proved that is capable of performing a $\Delta G/G$ measurement in three different ways. The results for the open charm and high–p_T analyses with $Q^2 > 1$ GeV^2 are still preliminary. For the former the optimisation of the RICH particle identification cuts is ongoing and the systematic errors are studied. For the latter the data from 2004 are processed and the optimisation of the cuts selecting the sample is being performed. The Neural Network approach is also considered here.

After a year break the COMPASS data taking is resumed in 2006. With a new target solenoid of a wider aperture [6], improvements in the RICH detector [18] and in the tracking system there should be a large improvement in the collected statistics.

References

[1] I. Balitsky, X. Ji.: Phys.Rev.Lett. **79** (1997) 1225.

[2] M. Hirai, S. Kumano, H. Saito: Phys. Rev. D **69** (2004) 054021.

[3] V. Yu. Alexakhin et al.: Phys. Lett. B (in press), hep-ex/0609038.

[4] A. Airapetian et al.: Phys. Rev. Lett. **84** (2000) 2584.

[5] B. Adeva et al.: Phys. Rev. D **70** (2004) 012002.

[6] M. Finger: these proceedings.

[7] G. Mallot: Nucl. Instrum. Meth. A **518** (2004) 121.

[8] C. Adloff et al.: Nucl. Phys. B **545** (1999) 21.

[9] G. Baum et al.: COMPASS proposal, CERN/SPSLC 96-14.

[10] A. Watson: Z. Phys. C **12** (1982) 123.

[11] M. Glück, E. Reya: Z. Phys. C **39** (1988) 569.

[12] A. Bravar, D. von Harrach, A. Kotzinian: Phys. Lett. B **421** (1998) 349.

[13] G. Ingelman: Comp. Phys. Comm. **101** (1997) 108.
[14] M. Glück, E. Reya, C. Sieg: Eur. Phys. J. C **20** (2001) 210.
[15] T. Sjöstrand et al.: Comp. Phys. Comm. **138** (2001) 238.
[16] E. S. Ageev et al.: Phys. Lett. B **633** (2006) 25.
[17] M. Glück, E. Reya, M. Stratmann, W. Vogelsang: Phys. Rev. D **63** (2001) 094005.
[18] E. Rocco: these proceedings.